Journal of
Materials Chemistry C

Accepted Manuscript

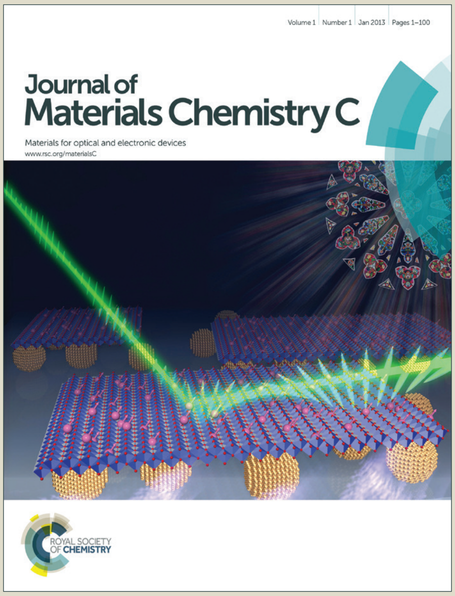

ROYAL SOCIETY OF CHEMISTRY

www.rsc.org/materialsC

Journal of Materials Chemistry C

RSCPublishing

COMMUNICATION

Cite this: DOI: 10.1039/x0xx00000x

Pressure-assisted electrode fabrication using simply synthesized Cu_3Sn alloy nanoparticles

Received 00th January 2012,
Accepted 00th January 2012

DOI: 10.1039/x0xx00000x

www.rsc.org/

Sanghun Cho[a], Keon-Hee Lim[a], Si Yun Park[a], Zhenxing Yin[a], Jeeyoung Yoo[a]* and Youn Sang Kim[a,b]*

Alloy nanoparticles have been widely investigated due to their unique properties and various applications. In particular, electrodes based on alloy nanomaterials can be good alternatives for advanced electrode fabrication due to their inherent, unique properties. Herein, we suggest a simple one-pot Cu_3Sn nanoparticles synthesis with high oxidation-resistivity, straightforward process-ability, and good electron conductivity. In addition, we introduce a pressure-assisted electrode fabrication at room temperature with the synthesized Cu_3Sn nanoparticles, which have a good potential for various functional devices on a plastic substrate.

Alloy nanoparticles have recently emerged as new attractive materials due to their advanced electrical, optical, magnetic, and catalytic properties when compared to the intrinsic properties of each of the elements.[1,2] Over the past several years, many researchers have been drawn to the synthesis method and noble-transition bimetallic or trimetallic alloy nanoparticles application due to their high catalytic performance or electrical properties.[3] Of these, silver or silver alloy nanoparticles have drawn interest because of their unique optical property, good oxidation-resistivity, low electron resistivity, etc. However, the high cost of silver or silver alloy nanostructures makes it difficult for utilization in various industrial applications.[4,5] On the other hand, as copper is abundant and has a relatively low cost, copper alloy nanoparticles have been introduced as an alternative to silver. For example, Cu_2ZnSnS_4 nanocrystals are promising for use as thin film solar cells due to the low cost, relatively low toxicity and appropriate optical properties (band-gap energy of ~1.5 eV).[6] Gold-Copper (Au_xCu_y) alloy nanoparticles also show stability and are tunable near infrared (NIR) emissions, which can be readily applied to biological analysis.[7]

Among various applications, the advanced electrode fabrication based on copper (Cu) nanoparticles has received a significant amount of attention due to the potential for use in ink jet printing or offset printing.[8,9] In particular, the Cu conductive nanoparticles have drawn interest due to the size effect of the melting point depression, which facilitates low temperature sintering for flexible electronics.[10] In addition, the nano-size electrode fabrication using conductive nanoparticles has a strong advantage; the simple printing process, which is better than conventional electrode fabrication like photolithography.[11] Cu nanoparticle ink has also good merits for repairing of disconnected electric wiring in electronic devices. Electrode fabrication using Cu nanoparticle ink is feasible for various applications, such as field effect transistor, solar cells, sensors, light emitting diodes, etc.[12,13] However, pure Cu nanoparticles have high reactivity that inevitably produce oxide layer during the purification process, storage in air condition, and sintering process for electrode fabrication.[14] The oxide layer of Cu nanoparticles has a negative effect on electrical resistivity, so cumbersome additional processes are needed to prevent its growth. For example, the sintering and storage of Cu nanoparticles require specific inert conditions, such as vacuum condition or nitrogen gas.[15] Additionally, the stabilizers for oxidation-resistivity, which are generally composed of organic materials, act as insulating layers on Cu nanoparticles. Therefore, they need a high decomposition temperature for use in conductive electrode fabrication, which limits the flexible substrates choices due to the thermal deformation of plastic materials.[16,17] In spite of the advantages of a simple electrode fabrication process using conductive ink based on Cu nanoparticles, these restrictions strongly inhibit applications in future flexible or wearable devices. Thus, alternative materials or processes for a low cost, high oxidation-resistivity, and low temperature fabrication are required.

To address these issues, we introduce a new Cu_3Sn alloy nanoparticles synthesis with good oxidation-resistance and the application for a pressure-assisted room temperature electrode fabrication. We synthesized the Cu_3Sn alloy nanoparticles of 60 nm average size with a highly oxidation-resistance using simple one-pot synthetic process. In the Cu_3Sn alloy nanoparticles synthesis, copper precursor, tin precursor, oleic acid, and oleylamine were used. The synthesized Cu_3Sn alloy nanoparticles did not change the electron resistivity during 4 weeks in ambient conditions. We successfully demonstrated the low electrical resistivity on flexible substrates *via* the pressure-assisted electrode fabrication with the synthesized Cu_3Sn alloy nanoparticles. The pressure on the Cu_3Sn alloy nanoparticles dramatically induced the interconnection between the neighboring Cu_3Sn alloy nanoparticles. As a result, in spite of the room temperature process, the electron resistivity of the Cu_3Sn alloy nanoparticles showed a value which is similar to that of conventional electrodes fabricated using pure copper or silver nanoparticle ink at a high temperature and inert gas sintering process.[18,19,20]

The Cu_3Sn alloy nanoparticles were synthesized by a thermal decomposition process in the presence of oleic acid and oleylamine. The precursors, copper (II) acetylacetonate and tin (II) acetylacetonate, were dissolved in an oleylamine and oleic acid mixed solution. The reaction mixtures were heated to 310 °C and aged for 1 hour. While the reaction was in process, the bright blue solution gradually changed colors to green, yellow, dark brown and then black, which represented the Cu_3Sn alloy nanoparticles formation. To remove the inorganic residues, the products were well washed using ethanol. The detailed Cu_3Sn alloy nanoparticles synthesis information is provided in the Experimental Section (Supporting Information).

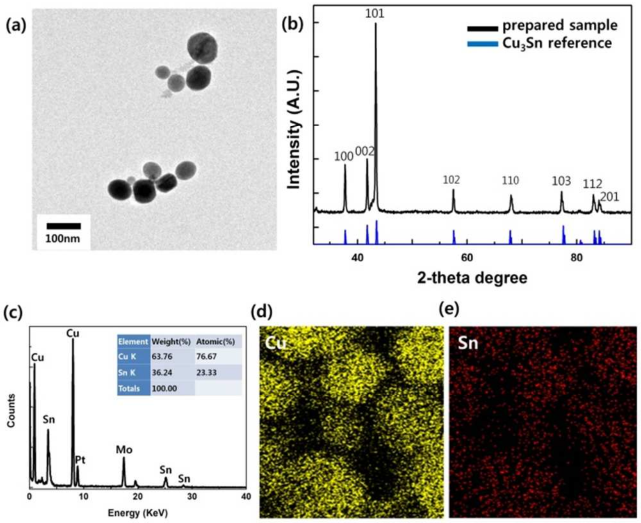

Element	Weight(%)	Atomic(%)
Cu K	63.76	76.67
Sn K	36.24	23.33
Totals	100.00	

Fig. 1. (a) TEM image of the synthesized Cu_3Sn nanoparticles with an average size of 60nm (b) XRD data of synthesized Cu_3Sn nanoparticles compared with Cu_3Sn reference peak (JCPDS 03-1010) (c) EDS spectrum of Cu_3Sn nanoparticles with Cu:Sn at 76.67:23.33 (d) The HAADF-STEM image and EDS mapping images of the Cu-Sn alloy (Cu_3Sn) nanoparticles.

The high resolution transmission electron microscopy (HRTEM) image in **Fig. 1a** shows the round shapes of the Cu_3Sn alloy nanoparticles. The HRTEM image reveals that they have an average size of 60 nm and the size distribution are depicted in Fig. S1. The X-ray diffraction (XRD) in Fig. 1b shows that the Cu_3Sn alloy nanoparticles have a typical Cu_3Sn reflection pattern (JCPDS 03-1010) in a dry powder sample. The major diffraction peaks at 2θ scattering angles agree with the hexagonal phase Cu_3Sn crystal. In Fig. S2, the lattice spacing of the Cu_3Sn alloy nanoparticles measure at 0.21nm corresponding to the (002) plane of Cu_3Sn and Selected Area Electron Diffraction (SAED) pattern indicates the crystal structure of the hexagonal Cu_3Sn phase. In addition, the Cu and Sn atoms ratio in the Cu_3Sn alloy nanoparticles is shown in Fig. 1c through the energy dispersive spectrometer (EDS) diagram. The Cu and Sn peaks are clearly observed in the spectrum except for the sputtering materials Pt and Mo signals in the TEM grid. To verify the molar ratio of Cu and Sn, scanning transmission electron microscopy (STEM)-EDS point spectra analysis was performed on the Cu_3Sn nanoparticle. It showed that the molar ratio of Cu and Sn was 76.7:23.3. The chemical compositions of the Cu_3Sn alloy nanoparticles are summarized in Table S1. We also conducted elemental distribution in the Cu-Sn alloy nanoparticles by carrying out an EDS elemental spectrum analysis with high angle annular dark-field scanning TEM (HAADF-STEM). Fig. 1d, e and S3 show the high resolution elemental mapping of the Cu_3Sn nanoparticles which are provided in the Cu (yellow) and Sn (red) distribution in each Cu_3Sn nanoparticle. These images confirm the well-distributed alloy state of the Cu_3Sn nanoparticles and show that there is no core-shell or uneven bimetallic structures in the Cu_3Sn nanoparticles. All

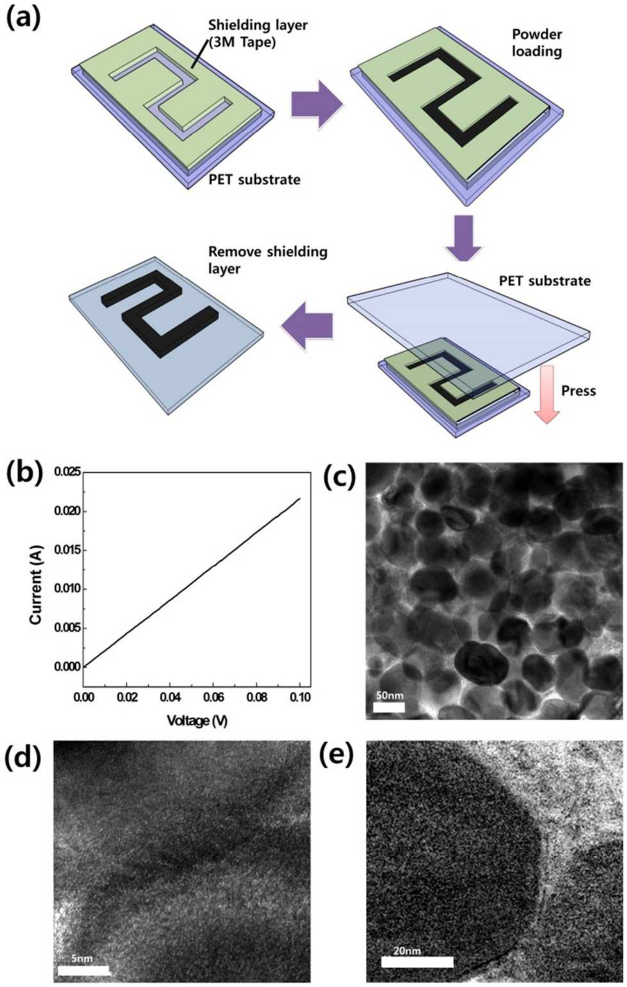

Fig. 2. (a) Schematic of pressure-assisted Cu_3Sn nanoparticle electrodes fabrication. (b) I-V curve of Cu_3Sn nanoparticles electrodes at a 131.3 MPa pressure condition, which correspond with conventional ohmic contact electron transport (c) Cross-sectional TEM images of pressed Cu_3Sn nanoparticle electrodes at 131.3 MPa pressure condition. (d) The enlarged cross-sectional TEM view of pressed Cu_3Sn nanoparticles. (e) TEM-EELS elemental mapping that show the carbon (white) elements.

images in Fig. 1 strongly confirm the homogeneous Cu_3Sn alloy nanoparticle formations.

Generally, the electrical resistivity of electrodes fabricated using nanoparticles is governed by two factors: the intrinsic metal resistivity and the residual surface layers induced by the capping agents. These affect the electron hopping and tunnelling, respectively.[21] The conductive metal nanoparticle core has many free electrons and act like bulk metal, which has a low electrical resistivity. Therefore, the residual surface layer induced by the capping agents is the most dominant factor in electron transport, so the electron transport mostly depends on the tunnelling phenomenon. Meanwhile, Shaowei Chen et. al. reported that the electrical characteristics of metal nanoparticle layers dramatically change in the "metallic ohmic contact" state by controlling the neighboring particle distance.[22,23] In that study, the simple linear I-V behaviour was observed when the neighboring particle distance was sufficiently small. This phenomenon implies that a small gap between adjacent nanoparticles can lead to electron hopping like metallic ohmic contact in electron transport between nanoparticles.

Based on the previous reports, we attempted to fabricate the conductive electrodes at room temperature using the pressure-assisted method with Cu_3Sn alloy nanoparticles. We assumed that the small gap between Cu_3Sn alloy nanoparticles induced by pressure on a sample could confirm electron hopping as with metallic ohmic contact in electron transport between Cu_3Sn alloy nanoparticles. This would considerably improve the electrical resistivity of the Cu_3Sn alloy nanoparticles layer. The fabrication method is detailed in **Fig. 2a**. A patterned shielding layer (3M tape) was first attached to the poly ethylene terephthalate (PET) substrate to prevent Cu_3Sn alloy nanoparticle powder spreading on unwanted space. The Cu_3Sn alloy nanoparticle powders were loaded on the patterned PET substrate and pressed for 3 min with a covered upper layer. After pressing, the shielding layer and upper layer were removed from the PET substrates. The conductive metal electrode pattern was well-developed in the flexible PET substrates.

The resistivity of the pressed Cu_3Sn alloy nanoparticles layers, ~ 19.8 μΩ·cm, is similar to that of the conventional conductive electrodes fabricated using pure copper or silver nanoparticles ink at a high temperature and inert gas sintering process. [18,19,20] Because the neighboring particle distance is small enough to result in metallic ohmic contact between the Cu_3Sn alloy nanoparticles, the pressed Cu_3Sn alloy nanoparticles resistivity is mainly determined by electron hopping. The pressure, which is a controlling factor for neighboring particle distance, induces the sequential transition by electron hopping and ultimately leads to the low electrical resistivity. To verify this assumption, we conducted current–voltage (I-V) characteristic and cross-sectional TEM analysis of the pressed Cu_3Sn nanoparticle layer. The I-V characteristics of the pressed Cu_3Sn layer at 131.3 MPa are shown in Fig. 2b. The linear shape indicates that the Cu_3Sn nanoparticle connections are very close enough to result in "metallic ohmic contact". Fig. 2c and S4 show the three-dimensional the pressed Cu_3Sn nanoparticles contact in bright and dark field cross-sectional TEM images. In particular, Fig. 2d shows the very close connections among neighboring Cu_3Sn nanoparticles. The residual carbon on the Cu_3Sn nanoparticles surface is traced by TEM-electron energy loss spectroscopy (EELS) element mapping, as shown in Fig. 2e. To ensure the fidelity of carbon element mapping by EELS, we verified the coincidence between the EELS spectrum of the carbon π* and σ* peak in Cu_3Sn nanoparticles and that of reference data. (Fig. S5) Elemental analysis of the carbon in Cu_3Sn nanoparticles confirms the carbon stabilizer distribution and shows that the carbon element is almost non-existent in the neighboring Cu_3Sn alloy nanoparticle interface. As a result, the pressure induced numerous three-dimensional close contact points among the Cu_3Sn nanoparticles and developed overall low electrical resistivity via metal ohmic contact.

The resistivity of the pressed Cu_3Sn nanoparticles layer is measured using a four-point probe method. **Fig. 3a** and Table S2 show the electrical resistivity of the pressed Cu_3Sn nanoparticles layers fabricated under various pressure conditions. The resistivity decreases from 25 μΩ·cm at 39.4 MPa to 19.8 μΩ·cm at 131.3 MPa. When the pressure exceeds 131.3MPa, the resistivity is saturated to approximately ~ 20 μΩ·cm, which is 2.2 times greater than the intrinsic resistivity of bulk Cu_3Sn (8.8 μΩ·cm). These results show that the electrical resistivity of the pressed Cu_3Sn nanoparticle layer is sufficiently low enough to behave as an electrical conducting layer (electrode), even though the pressed layer is developed at room temperature. Many ink jet printing studies on Ag and Cu nanoparticles have reported that the resistivity is between 5 ~ 40 μΩ·cm at a sintering temperature from 150 °C to 400 °C.[18,19,20] Although the resistivity of bulk Ag (1.47 μΩ·cm) and Cu (1.7 μΩ·cm) is five to six times lower than that of the bulk Cu_3Sn, the resistivity of the conductive pattern fabricated by pure Cu or Ag nanoparticle ink shows that are similar to that of the pressed Cu_3Sn nanoparticle electrode.

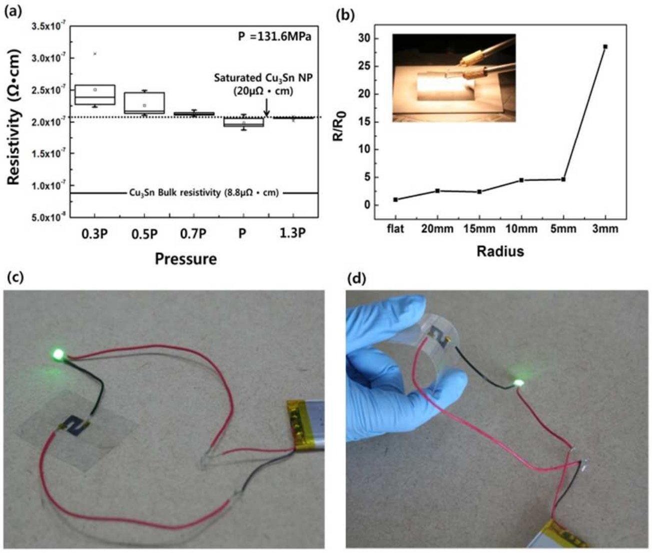

Fig. 3. (a) Electrical resistivity of the pressed Cu_3Sn nanoparticles electrode as a function of pressure. The Cu_3Sn nanoparticles electrodes were fabricated at various pressures ranging from 39.4 MPa to 170.7 MPa. (b) Electrical resistivity of the pressed Cu_3Sn nanoparticles electrodes with varying bend radius, and a bending measurement image (inset). Optical images of the Cu_3Sn nanoparticles electrode pattern in a (c) flat state and (d) bent state.

In addition, the pressed Cu_3Sn nanoparticle electrode could be formed on flexible substrates like plastic or paper substrates because the fabrication process only requires a simple pressing process at room temperature. Furthermore, the numerous neighboring particle contacts of pressed Cu_3Sn nanoparticle electrode confirm the low resistivity at various bending states. We measured the resistivity at various bending conditions to show the potential as a flexible electrode. The bending test scheme shows Fig. S6 and the bending results in Fig. 3b reveal that except for the deformed state at 3 mm radius, the flexible test is reliable for the electrodes until 5 mm radius. At 20 mm radius and 15 mm radius, the relative resistivity is twice the flat resistivity. When the radius reaches 10 mm and 5 mm, the relative resistivity becomes three times greater than the flat resistivity. At 3 mm radius, the values abruptly increase to 30 times due to the pressed Cu_3Sn nanoparticle interconnection tearing. Fig. 3c and Fig. 3d show the optical photographs of the Cu_3Sn electrodes fabricated by this pressure-assisted method. The images indicate the presence of well-patterned electrodes on the flexible PET substrate, which are electron-conductive enough to turn on bright LEDs. For the micro-scale phase observation of the pressed Cu_3Sn electrodes, we analyzed the pressed Cu_3Sn electrodes using the cross-sectional Scanning Electron Microscopy (SEM) images (Fig. S7). The SEM image shows that the Cu_3Sn electrodes have well-packed layers with densely inter-contacted Cu_3Sn nanoparticles.

To verify the flexible characteristics between neighboring Cu_3Sn alloy nanoparticles, the pressed electrode bending test is performed at a bending radius of 15mm. The pressed electrode shows good mechanical stability with a nearly constant resistivity as shown in Fig. S8. In addition, we demonstrated the re-connecting of the disconnected electric wires (Fig. S9). Fig. S9a, S9c images show the disconnected electric wire and Fig. S9b, S9d images show the reconnected electric wire by the pressure assisted electrode fabrication with Cu_3Sn nanoparticles. These results represent potentially viable the pressure assisted electrode fabrication with Cu_3Sn nanoparticles in re-connecting disconnected wires.

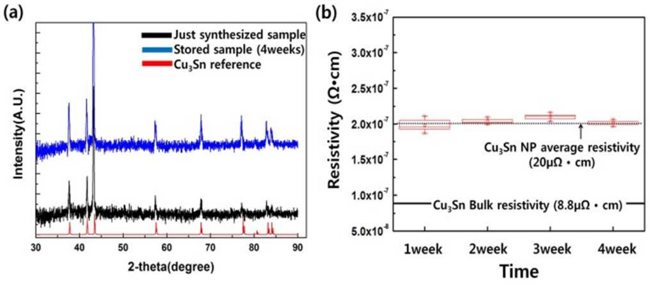

Fig. 4. (a) XRD patterns of the synthesized Cu_3Sn alloy nanoparticles; just fabricated and stored in ambient air conditions (RH 50%, 25 °C) for 4 weeks (b) The resistivity variation of the electrodes fabricated by pressured Cu_3Sn alloy nanoparticles corresponding to the stored time in ambient air conditions

Finally, we verified the good oxidation-resistivity of the Cu_3Sn nanoparticles during 4 weeks. The oxidation-resistance of the Cu_3Sn alloy has been reported to be higher than that of Cu in its bulk material state.[24] Although nanostructured materials have somewhat different characteristics from bulk materials, we could easily assume that the oxidation-resistance trend was similar. To show the good oxidation-resistivity of the alloyed Cu_3Sn nanoparticles, the pressed Cu_3Sn nanoparticles electrode resistivity was monitored for 4 weeks under 50% relative humidity at 25 °C. (**Fig. 4**) The XRD analysis in Fig. 4a indicates that the copper oxide and tin oxide peaks are almost non-existent even after 4 weeks. However, the metal nanoparticle has generally an amorphous oxide layer and the synthesized Cu_3Sn alloy nanoparticles also have an native oxide layer.(See Fig. S10) Although the Cu_3Sn alloy nanoparticles have an oxide layer that is less than a few nanometers, the oxidation characteristics are considerably different when with Cu nanoparticles. The native oxide layers of the Cu nanoparticle diffuse into internal crystal structures. The diffused oxygen in Cu nanoparticles deform the intrinsic crystal structures like copper oxide and hollow structures.[25,26,27] However, Cu_3Sn alloy nanoparticles shows constant oxygen ratio in EDS analysis (Fig. S11a, S11b) and constant crystal structure in the SAED pattern (Fig. S11c, S11d) irrespective of storage time for 4 weeks. Furthermore, Fig. 4b and Table S3 show the constant resistivity of the pressed Cu_3Sn nanoparticle electrodes even after 4 weeks. These results reveal that the oxidation-resistance of the Cu_3Sn alloy nanoparticles is superior to that of the pure Cu nanoparticles. [25,26,27]

Conclusion

In conclusion, we introduced a new synthesis of the high oxidation-resistance of Cu-Sn alloy (Cu_3Sn) nanoparticles using a simple one-pot reaction. The synthesized Cu_3Sn nanoparticles had an average diameter of 60 nm. Compared to Cu, Ag, and other nanoparticles, the Cu_3Sn nanoparticles had the promising electrode properties such as oxidation-resistivity, low cost materials, simple process-ability, and room temperature electrode fabrication-ability, as an electrode material. In particular, the Cu_3Sn nanoparticles did not show appreciable oxide impurities even when left in contact with air for 4 weeks under ambient conditions (RH 50%, 25 °C). The electrical resistivity of the pressed Cu_3Sn nanoparticles layer also showed little change after 4 weeks. This oxidation-resistance confirmed that the Cu_3Sn nanoparticles could easily be used for electrode materials without needing any cumbersome storage conditions. In addition, we introduced a pressure-assisted electrode fabrication method using Cu_3Sn nanoparticles, which has suitable electrical resistivity for a conductive line. The electrical resistivity of the pressed Cu_3Sn nanoparticles electrode was 19.8 $\mu\Omega\cdot$cm at 131.3 MPa. Consequently, we confirmed that the pressure considerably helps connect the Cu_3Sn nanoparticles at room temperature and effectively induces low electrical resistivity in Cu_3Sn nanoparticle electrodes. This pressure-assisted electrode fabrication technique has several advantages over previous printing fabrications. The fabrication does not require any cumbersome processes such as the ink formulations optimization with viscosity, solids content, and solvent type. There are also potential cost advantages due to the use of low cost materials and simple non-vacuum processing conditions. Furthermore, room temperature fabrication enables the use of flexible devices based on plastic substrates. We believe that the high oxidation-resistance of Cu_3Sn alloy nanoparticle synthesis and the pressure-assisted electrode fabrication process induce a leap in conventional electrode fabrication methods and they have good potential for various functional devices on a plastic substrate.

Acknowledgement

This work was supported by Basic Research Program (2011-0018113) and Center for Advanced Soft Electronics under Global Frontier Research Program (2013M3A6A5073177) of National Research Fund (NRF) by Korea.

Notes and references

[a] Program in Nano Science and Technology, Graduate School of Convergence Science and Technology, Seoul National University, Seoul 151-742, Korea
E-mail: younskim@snu.ac.kr
[b] Advanced Institutes of Convergence Technology, lui-dong 864-1 Yeoungtong-gu, Suwon-Si, Gyeonggi-do 443-270, Korea

† Footnotes should appear here. These might include comments relevant to but not central to the matter under discussion, limited experimental and spectral data, and crystallographic data.

Electronic Supplementary Information (ESI) available: [details of any supplementary information available should be included here]. See DOI: 10.1039/c000000x/

1 S. Alayoglu, A. U. Nilekar, M. Mavrikakis, B. Eichhorn, *Nat. Mater.,* 2008, **7**, 333-338.
2 S. H. Zhou, B. Varughese, B. Eichhorn, G. Jackson, K. McIlwrath, *Angew. Chem. Int. Edit.,* 2005, **44**, 4539-4543.
3 D. S. Wang, Y. D. Li, *J. Am. Chem. Soc.,* 2010, **132**, 6280-6281.
4 S. Link, Z. L. Wang, M. A. El-Sayed, *J. Phys. Chem. B.,* 1999, **103**, 3529-3533.
5 H. Jiang, K. S. Moon, F. Hua, C. P. Wong, *Chem. Mater.,* 2007, **19**, 4482-4485.
6 Q. J. Guo, H. W. Hillhouse, R. Agrawal, *J. Am. Chem. Soc.,* 2009, **131**, 11672-11673.
7 C. M. Andolina, A. C. Dewar, A. M. Smith, L. E. Marbella, M. J. Hartmann, J. E. Millstone, *J. Am. Chem. Soc.,* 2013, **135**, 5266-5369
8 S. Jeong, H. C. Song, W. W. Lee, S. S. Lee, Y. Choi, W. Son, E. D. Kim, C. H. Paik, S. H. Oh, B. H. Ryu, *Langmuir,* 2011, **27**, 3144-3149.
9 J. Perelaer, P. J. Smith, D. Mager, D. Soltman, S. K. Volkman, V. Subramanian, J. G. Korvink, U. S. Schubert, *J. Mater. Chem.,* 2010, **20**, 8446-8453.
10 D. L. Schodek, P. Ferreira, M. F. Ashby, Nanomaterials, nanotechnologies and design: an introduction for engineers and architects, Butterworth-Heinemann, **2009**.
11 J. S. Kang, H. S. Kim, J. Ryu, H. T. Hahn, S. Jang, J. W. Joung, *J. Mater. Sci.: Mater. Electron.,* 2010, **21**, 1213-1220.
12 S. Gamerith, A. Klug, H. Scheiber, U. Scherf, E. Moderegger, E. J. W. List, *Adv. Funct. Mater.,* 2007, **17**, 3111-3118.
13 M. Grouchko, A. Kamyshny, S. Magdassi, *J. Mater. Chem.,* 2009, **19**, 3057-3062.
14 S. Magdassi, M. Grouchko, A. Kamyshny, *Materials,* 2010, **3**, 4626-4638.
15 C. Kind, A. Weber, C. Feldmann, *J. Mater. Chem.,* 2012, **22**, 987-993.
16 Z. C. Xu, C. M. Shen, Y. L. Hou, H. J. Gao, S. S. Sun, *Chem. Mater.,* 2009, **21**, 1778-1780.
17 V. Zardetto, T. M. Brown, A. Reale, A. Di Carlo, *J. Polym. Sci. Pol. Phys.,* 2011, **49**, 638-648.
18 Z. L. Zhang, X. Y. Zhang, Z. Q. Xin, M. M. Deng, Y. Q. Wen, Y. L. Song, *Nanotechnology,* 2011, **22,** 425601-425608.
19 K. Ankireddy, S. Vunnam, J. Kellar, W. Cross, *J. Mater. Chem. C,* 2013, **1**, 572-579.
20 Y. Lee, J. R. Choi, K. J. Lee, N. E. Stott, D. Kim, *Nanotechnology,* 2008, **19,** 415604-415611.
21 C. P. Collier, T. Vossmeyer, J. R. Heath, *Annu. Rev. Phys. Chem.,* 1998, **49**, 371-404.
22 S. W. Chen, *J. Mater. Chem.,* 2007, **17**, 4115-4121.
23 S. Pradhan, J. Sun, F. J. Deng, S. W. Chen, *Adv. Mater.,* 2006, **18**, 3279-3283.
24 H. Liu, K. Wang, K. Aasmundtveit, N. Hoivik, in Electronic Components and Technology Conference (ECTC), 2010 Proceedings 60th, IEEE, **2010**, 853-857.
25 M. Yin, C. K. Wu, Y. B. Lou, C. Burda, J. T. Koberstein, Y. M. Zhu, S. O'Brien, *J. Am. Chem. Soc.,* 2005, **127**, 9506-9511.
26 M. Salavati-Niasari, F. Davar, *Mater. Lett.,* 2009, **63**, 441-443.
27 S. U. Son, I. K. Park, J. Park, T. Hyeon, *Chem. Commun.*, 2004,**7**, 778-779.

Pressure-assisted electrode fabrication using simply synthesized Cu3Sn alloy nanoparticles

Sanghun Cho[a], Keon-Hee Lim[a], Si Yun Park[a], Zhenxing Yin[a], Jeeyoung Yoo[a]* and Youn Sang Kim[a,b]*

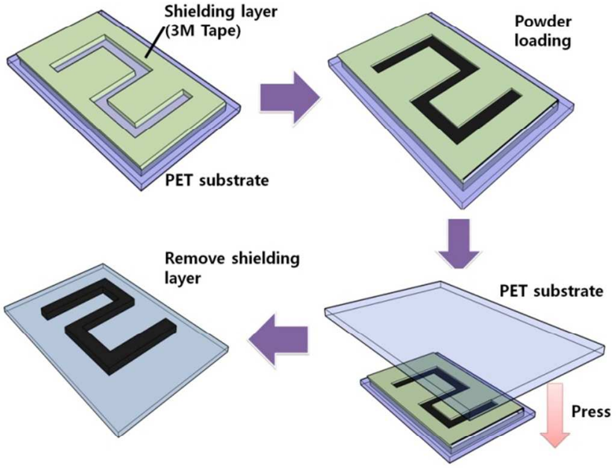

Herein, we suggest the simple one-pot synthesis of Cu_3Sn nanoparticles with high oxidation-resistivity, easy process-ability and good electron conductivity. In addition, we introduce the fabrication of pressure-assisted electrode at room temperature with the synthesized Cu_3Sn nanoparticles, which have a good potential for various functional devices on a plastic substrate.